Interface energetics in zinc phthalocyanine growth on Ag(100)

Abdullah Al-Mahboob[1,2] and Jerzy T. Sadowski[1,*]

[1]*Center for Functional Nanomaterials, Brookhaven National Laboratory, Upton, New York 11973, USA*

[2]*Department of Physics, University of Liverpool, Liverpool L69 3BX, United Kingdom*

(Received 2 November 2015; published 8 February 2016)

The nucleation and growth of zinc phthalocyanine (ZnPc) thin films on a Ag(100) surface are studied employing *in situ*, real-time low-energy electron microscopy and complementary density functional theory (DFT) calculation to elucidate the role of incorporation kinetics of planar molecules in phase selection during nucleation and apply this knowledge to the fabrication of highly crystalline ZnPc films. We show that the nucleation of crystalline ZnPc islands requires a large concentration of diffusing molecules. The required amount of nominal deposition to initiate the growth of monolayer (ML) high two-dimensional crystalline islands is dependent on both growth temperature and crystalline phase. At room temperature (RT) and slightly above (RT to ∼430 K), ZnPc crystalline islands have double-domain *R*33.69 structures with average domain sizes in the submicrometer range. At higher temperatures, a 5 × 5 commensurate ZnPc structure nucleates. DFT calculations reveal significant differences in interfacial energies of an isolated ZnPc molecule on a substrate, depending on an adsorption site and azimuthal orientation of the molecule relative to the substrate atomic lattice. The observed delay in the onset of the nucleation of an island is caused by the existence of a large energy barrier for molecule incorporation into an island. At certain growth conditions it is possible to induce a structural transition from the 5 × 5 to the *R*33.69 phase when the nominal coverage reaches 1 ML. The resulting film has excellent crystallinity with individual domains of hundreds of micrometers in size.

DOI: 10.1103/PhysRevB.93.085413

I. INTRODUCTION

Multidisciplinary research in organic molecular films draws significant attention due to synthetic flexibility, diverse functionality, and progress in the field of organic devices, offering a potential for low cost facile manufacturing. Among organic molecules, metal phthalocyanines (MPcs) are of continued interest as they find both technological and scientific attention [1], being successfully used in various applications, such as plastic electronics [2], chemical sensors [3], and solar cells [4], to name a few. Metal phthalocyanines belong to a class of macrocyclic compounds with four nitrogen atoms which act as coordination centers for a metal ion within the central cavity of the MPc molecule. Pcs form complexes with a majority of elements in the periodic table [5], and thus they offer great flexibility for tuning their properties via changing the center metal ion and/or inserting different chemical end groups in the molecule. The metal centers in MPcs introduce various functionalities that make them useful in catalysis [6–8], gas sensing [9–11], and molecular magnetism applications [12]. Moreover, one of the most important advantages of phthalocyanines over other organic materials is their exceptional thermal and chemical stability. Thin films can therefore readily be prepared by organic molecular-beam epitaxy in vacuum [13].

Unlike inorganic semiconductors in which the interatomic forces arise from strong covalent or ionic bonds, MPc molecules are held together in a crystal or molecular film by weak van der Waals forces. This produces a variety of metastable polymorphs, depending on the preparation conditions of the film [1,14–16]. In addition to the intermolecular interactions, film morphology is determined by the details of the interactions of the molecules with the substrate. The shape anisotropy of a planar molecule, such as phthalocyanine is expected to make its aggregation processes complex in a similar fashion to film growth of other anisotropic molecules [17–20]. Moreover, the metal center is accessible from both sides of the molecular plane. Therefore, a choice of metal center in the molecule determines not only the chemical functionality, but also opens the way for manipulating the interplay between molecule-molecule and molecule-substrate interactions and thus controlling the resulting structure of a molecular film. For instance, 1 ML of CoPc grown on a Ag(100) surface at room temperature (RT) is reported to have a 5 × 5 commensurate structure with a substrate lattice [21], whereas ZnPc on Ag(100) has been reported to have a double-domain structure [22]. Moreover, a gas-phase (diffusing phase) CuPc on a Au(111) surface at RT below 0.93 ML coverage and on Cu(111) below 0.76 ML coverage, respectively, are also reported [23]. In the present paper, we examine the film growth of a metal Pc in relation to attachment-detachment kinetics for manipulating nucleation, phase transition, and crystalline structures. In our primary study, we have deposited a number of metal Pcs on various substrates (oxides, graphene, and fourfold and threefold metal surfaces). Among these we have selected ZnPc and a fourfold Ag(100) surface for extensive investigation as a model system in which both, double domain and 5 × 5 commensurate structures, are reported for RT-grown MPcs with Zn and Co metal centers, respectively. Another reason of choosing the (100) surface is that both substrate and molecule have square symmetry. The MPc is a planar rigid molecule, consisting of a large number of atoms (57), strongly interacting with Ag surfaces [1]. Upon incorporation into a crystalline film, the molecule must assume a specific orientation, and thus we expect that the anisotropy in rigid atomic arrangements and the atomic bonding configuration within the molecule will result in a reorientation limited mechanism governing the growth of a crystalline film [17–20].

*sadowski@bnl.gov

II. EXPERIMENTAL AND COMPUTATIONAL PROCEDURES

In this paper we applied low-energy electron microscopy (LEEM) [24] as a main experimental technique, whereas complementary density functional theory (DFT) calculations were employed for a better understanding of the experimentally observed phenomena. LEEM and selected-area low-energy electron diffraction (μ-LEED) measurements were performed at the Elmitec SPE-LEEM system situated at beamline U5UA of the National Synchrotron Light Source. ZnPc was thermally evaporated on a single-crystal Ag(100) substrate in the LEEM system under ultrahigh vacuum with a base pressure in the range of $\sim 5 \times 10^{-10}$ Torr at deposition rates ranging from 0.03 to 0.05 ML min. The molecular flux was calibrated monitoring the nominal deposition required for a full ML coverage of crystalline islands and further verified observing the additional nominal deposition required for completion of a second layer. Here, 1 ML corresponds to 5.2×10^{17} molecules cm^{-2}—the molecular density of a single-crystalline layer composed of lying down ZnPc molecules at room temperature [22] that fully cover the Ag(100) surface. The substrate temperatures were varied from RT to 520 K, depending on the experiment.

In order to better understand experimental results, the site-dependent and orientation-dependent interface energies of the ZnPc molecules on Ag(100), in-plane molecule-molecule binding energies (BEs), and molecule-molecule interfacial energies were computed employing DFT. The DFT electronic structure program materials studio Dmol^3 [25,26] has been employed. Geometry optimization and dispersion correction for DFT (DFTD) [generalized gradient approximation (GGA) + dispersion correction] energy calculations were carried out by using the Perdew-Burke-Ernzerhof GGA functional [27], and the van der Waals correction was accounted for by employing the DFTD method by Grimme [28] using the DFT semiempirical dispersion interaction correction module [29]. The relativistic correction [30,31] was employed using the DFT semi-core pseudopotential (DSPP) [32]. The energies were calculated also for the optimized structure at local minima in which the azimuthal orientation and the adsorption site of molecules were constrained.

The optimized adsorption site and molecule orientation for an isolated molecule was determined by placing it on a large four-atomic-layer-thick Ag(100) supercell (8×8) and subsequent geometry optimization. The interfacial energies were also calculated for the experimentally observed commensurate structure (5×5 phase). We did not perform similar calculations for the $R33.69$ phase as a much larger unit cell for adsorption structure made the calculations not feasible. In order to get the relative interfacial energies, we have computed DFTD binding energies of isolated ZnPc molecules on Ag(100) with various azimuthal orientations and their possible adsorption sites.

III. RESULTS AND DISCUSSION

We have studied the structural evolution of zinc phthalocyanine (ZnPc) thin films on a Ag(100) single crystal, which can be regarded as a model system for phthalocyanine growth as we mentioned above. We utilized in investigating real-time nucleation, film growth, and phase-transition varying substrate temperatures to elucidate how the energy barriers for incorporation (molecule diffusion and reorientation) affect the nucleation, growth, and the resulting structure of the molecular film.

Upon deposition of the ZnPc molecules on the Ag(100) surface, we observed that a substantial nominal coverage of molecules is required before onset of the formation of a crystalline ZnPc layer similar as the reported ordered structure is determined by LEED upon coverage of CuPc over 0.76 and 0.93 MLs on Cu(111) and Au(111) surfaces, respectively [23]. A series of LEEM images recorded during deposition of ZnPc on Ag(100) kept at 375 K is shown in Fig. 1. Note that at this temperature the onset of nucleation of a crystalline ZnPc layer, manifested by the appearance of "bright" islands in LEEM images, was observed at a nominal coverage of 0.33 ML. The μ-LEED pattern taken from the surface depicted in the first LEEM frame [(Fig. 1(a)] is shown in Fig. 1(d). The high background around the (00) diffraction spot and very faint diffraction features indicate that molecules are in a gas phase or transient state (transitional short-range order) before the onset of the nucleation of the crystalline islands. Once they nucleate, the 1 ML high ZnPc islands have well-defined crystalline structures, and they are epitaxially aligned with the Ag(100) substrate as can be seen in Figs. 1(e) and 1(f). From comparing these two LEED patterns it also becomes immediately apparent that changing the growth temperature results in different crystalline structures of the islands.

A more detailed analysis of the LEED patterns revealed that at a growth temperature of 375 K the ZnPc film nucleates with the double-domain structure similar to the one reported by Dou *et al.* [22]. Both the LEEM data and the μ-LEED pattern, which was obtained with a 2 μm selected-area aperture [Fig. 2(a)] show that the individual domains are of submicrometer size. We utilized a LEED pattern recorded from a clean Ag(100) surface, shown in Fig. 2(c) as a reference for the analysis of the ZnPc in-plane epitaxial structures. Every third ZnPc molecule matches its relative position with an underneath Ag atom resulting in a unit cell (denoted subsequently $R33.69$) with respect to the shortest Ag surface lattice vector described by Ag$[0\ \frac{1}{2}\ \frac{1}{2}]$ and Ag$[0\ -\frac{1}{2}\ \frac{1}{2}]$. The above-described structure is obtained when the ZnPc film is grown on a substrate kept at temperatures from RT to approximately 445 K.

When the substrate temperature exceeds 445 K, a different LEED pattern is obtained as shown in Fig. 2(b). From the analysis of this pattern it is apparent that all the ZnPc islands have single commensurate orientation but with about 4% larger in-plane lattice vectors (nearest-neighbor distance of $a = 14.445$ Å) in comparison with the double-domain structure (nearest-neighbor distance of $a = 13.89 \pm 0.092$ Å). A lower molecular density of the 5×5 commensurate structure indicates that this is a substrate-induced structure. There, the position of neighboring ZnPc molecules matches with every fifth Ag atom along the shortest surface lattice vectors Ag$[0\ \frac{1}{2}\ \frac{1}{2}]$ or Ag$[0\ -\frac{1}{2}\ \frac{1}{2}]$. In further considerations we will label this phase as a 5×5 phase.

As mentioned above, in real-time LEEM experiments we observe long delay in the nucleation of crystalline ZnPc islands. The nominal coverage of ZnPc molecules required

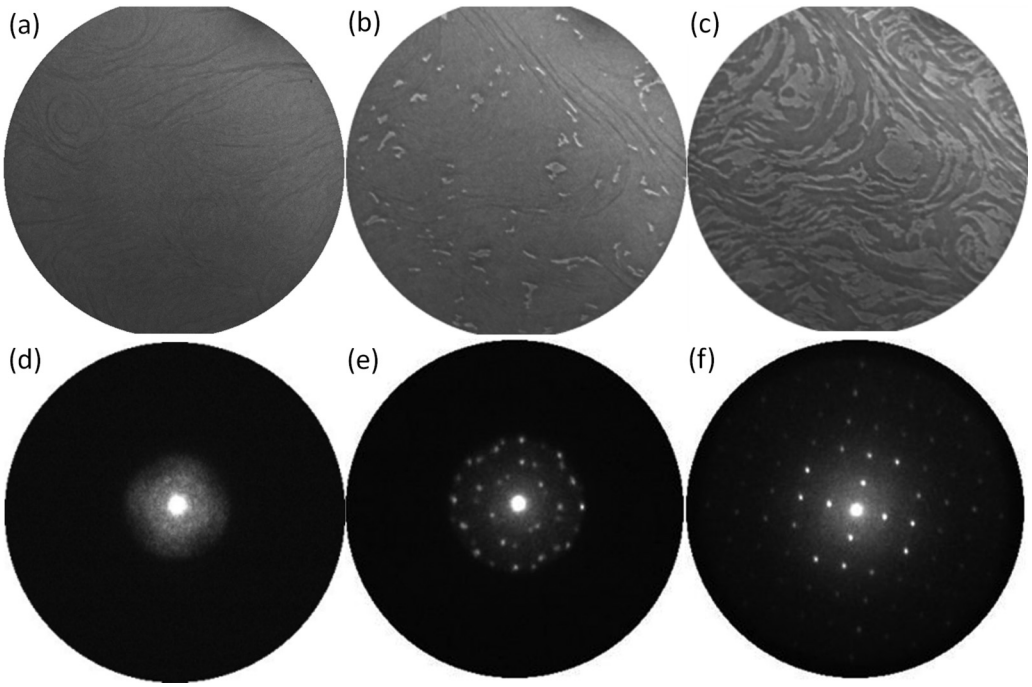

FIG. 1. (a)–(c) Time-series LEEM images obtained during the growth of ZnPc on Ag(100) at 375 K: (a) before nucleation of the crystalline islands at nominal coverage of 0.3 ML, (b) right after nucleation—0.35 ML, (c) at 0.7 ML nominal coverage; field of view 10 μm; $E = 2.5$ eV, and (d) and (e) μ-LEED patterns recorded during the growth of ZnPc: (d) before an onset of the nucleation of the crystalline islands (0.3 ML) at 375 K, $E = 2$ eV, (e) from 1 ML ZnPc crystalline islands grown at 375 K, $E = 4$ eV, and (f) from 1 ML ZnPc crystalline islands grown at 460 K, $E = 25$ eV.

to be on the substrate for the onset of nucleation increases with a rise in substrate temperature. This critical coverage equals 0.33 ML at 375 K, and it is as much as 0.87 ML at 520 K. In the literature, such a delay in the formation of an ordered layer is reported and described in terms of the interplay of intermolecular interaction and a large gas-phase concentration of molecules. In some specific cases, the high concentration of gas phase is explained in terms of repulsive-attractive interaction versus intermolecular spacing at gas-phase molecules [33]. However, those studies of the delayed nucleation of the ordered structure and prior high concentration of gas-phase molecules [23,33] are lacking information about the concentration of diffusing molecules within the region in between crystalline islands after nucleation and during subsequent growth to complete a monolayer. As the LEEM allows for obtaining spatially resolved information in real time, we were able to monitor the coverage of the crystalline islands as a function of total nominal deposition at given temperatures and deposition rates. The relation between nominal deposition and actual coverage of the crystalline islands for these two temperatures is shown in Fig. 3. Interestingly, as we see in Fig. 3, the island grows faster than the deposition rate, but the coverage proceeds linearly with time after nucleation such that the gas-phase concentration in between islands remains constant. This observation suggests a large critical concentration of gas-phase molecules which are in kinetic

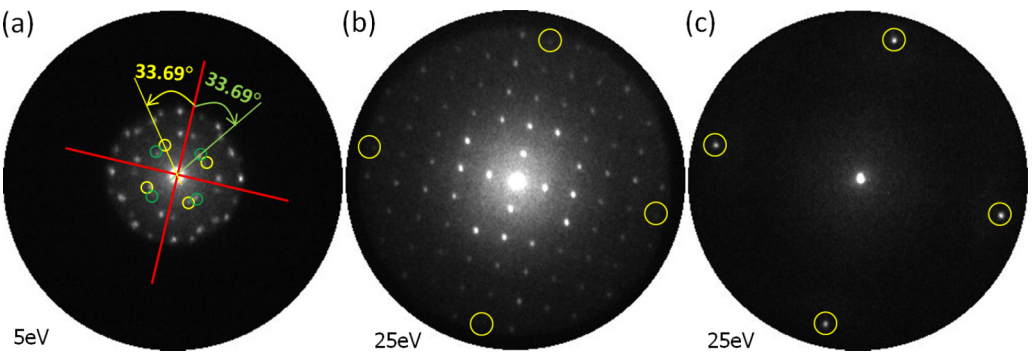

FIG. 2. μ-LEED patterns obtained from ZnPc crystalline islands grown at various temperatures: (a) the double-domain $R33.69$ phase grown at 375 K with orientations of two domains outlaid on the pattern, (b) the single-crystalline 5×5 phase grown at 460 K, and (c) the LEED pattern from a clean Ag(100) surface as a reference—Ag(100) first-order diffraction spots are marked by yellow circles in (b) and (c). The size of the selected-area aperture for μ-LEED was 2 μm.

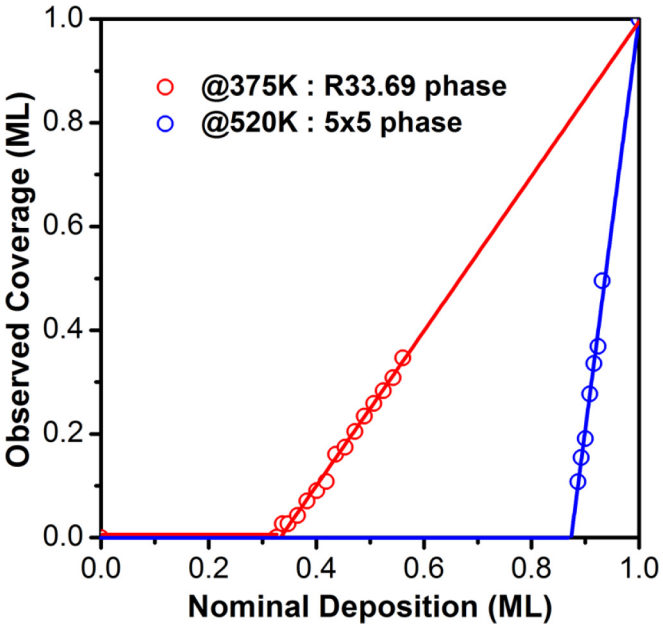

FIG. 3. Coverages of ZnPc crystalline phases versus nominal deposition, extracted from real-time LEEM observations of ZnPc deposition on Ag(100) at substrate temperatures of 375 and 520 K, respectively.

equilibrium with the crystalline islands due to the balance between attachment and detachment processes.

If ZnPc is deposited on a substrate kept at higher temperatures (HTs), nucleation of the ordered island requires a larger amount of nominal deposition. Therefore, one could speculate that the increase in critical coverage with the temperature is partially caused by desorption of ZnPc molecules at elevated substrate temperatures. This is not the case, however, as confirmed from both DFT calculation and the real-time LEEM experiments. A schematic landscape of relative interfacial energies obtained from DFT calculations is outlined in Fig. 4. DFT-calculated interface energy per molecule between a molecule and a Ag(100) surface is found to be 6.84 eV. Therefore we do not expect any desorption at the growth temperatures presented in Fig. 3. Moreover, we observed that virtually the same nominal coverages (accounting for differences in the surface density of $R33.99$ and 5×5 phases) were required to grow full MLs of ZnPc. This supports our claim that there is no noticeable desorption of the ZnPc molecules at the range of substrate temperature employed. Reiterating, in the initial stages of the ZnPc deposition there is a large number of diffusing ZnPc molecules on the surface, which are in kinetic equilibrium (balancing kinetic attachment and thermal detachment against the BE of molecules at the edge of the nucleated island) with the nucleating island. In such a case, the critical density required for the onset of nucleation should depend on the substrate temperature, and this relation should be governed by an Arrhenius-type activation of detachment processes.

In classical nucleation and island growth theory, it is assumed that an adatom is attached immediately at an island edge just upon arrival. In the case of a molecular system where the molecule has a different orientation in the diffusing state than in the crystalline state, if molecules require overcoming a large orientation barrier, it can result in a slow incorporation. In such cases, therefore, we have treated the problem in terms of an incorporation-limited model in which the molecules need to reorient themselves from time-averaged orientations in the diffusing state to the one that matches the orientation of a molecule in the crystalline phase. This introduces an attachment barrier E_{at}. In our previous reports on the growth of films made of anisotropic molecules [20,34] where the molecules prefer to be at different orientations at a diffusive state (lying down) than that in crystalline islands (standing up), we found that the energy barrier for molecule

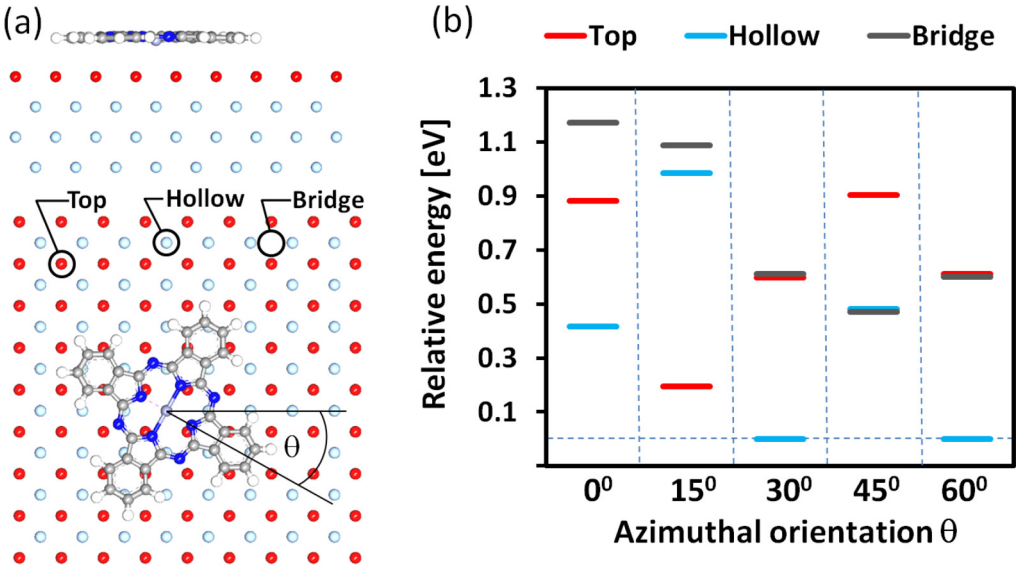

FIG. 4. (a) Side and top views of a ZnPc molecule adsorbed on Ag(100) with schematics of adsorption geometry and possible adsorption sites considered in calculations and (b) a diagram of calculated binding energies of ZnPc molecules having different azimuthal orientations and adsorption sites as marked in (a); a hollow site with $\pm 30^{\circ}$ rotation of the molecular axis with regard to the [011] axis of the substrate is a preferred adsorption configuration.

reorientation causes a delay in the nucleation of the crystalline islands. In that experimental system the incorporation-limited growth model was proposed. In the case of MPcs on metal surfaces, molecules are lying down in both the gas phase and the crystalline state as this configuration maximizes total molecule-substrate interaction. However, the molecule should have a specific orientation in a crystalline film. We cannot exclude the existence of an energy barrier for molecule attachment in the growth of a crystalline film, which originates from variation in interfacial energy depending on the azimuthal orientation of the molecule. In fact, DFT calculation shows remarkable differences up to few hundred meV in both the site-dependent and the orientation-dependent BEs as shown in Fig. 4(b). ZnPc molecules prefer to adsorb on hollow sites in the Ag(100) lattice with the molecular axis rotated about $\pm 30°$ with regard to the [011] crystallographic direction of the substrate. This is in agreement with scanning tunneling microscopy data obtained from NiPc and CoPc molecules adsorbed on Ag(100) [35]. Molecule-substrate interaction (6.84 eV per molecule obtained from DFT calculation for a commensurate polymorph) is much stronger than the in-plane molecule-molecule interaction: 0.17 eV for the 5×5 phase, 0.28 eV for the $R33.69$ phase (without considering the substrate in the calculations). It is also stronger than out-of-plane molecule-molecule interaction (0.94 eV). Increases in interfacial energies upon a change in azimuthal orientation from 30° to 15° and 30° to 45° at a hollow site are 0.99 and 0.48 eV, respectively. The actual energy barrier for azimuthal reorientation should be larger than that as the reorientation process should occur through local transitional states. We can thus conclude that the reorientation barrier associated with the anisotropy of a molecular structure can be a prime factor over molecule-molecule interaction. This implies that an energy barrier for molecule reorientation should be considered in the analysis of film nucleation and growth. DFT calculations of site- and orientation-dependent adsorption energies of ZnPc molecules suggest a large effective energy barrier for a molecule being incorporated into a nucleus or an island. The nucleation and film growth should be considered in terms of incorporation-limited kinetics. In such a growth mechanism, only a fraction of molecules is attached upon their arrival at an island edge. Therefore, the concentration of gas-phase molecules at kinetic equilibrium is determined by the balance of a slow attachment and thermal detachment processes.

Neglecting the effect of deposition rate, a simplified rate of attachment R_{at} in this incorporation-limited mechanism can be given as

$$R_{at} = \frac{1}{2}\rho\, p_a a \nu_{\text{diff}} \exp\left(-\frac{E_{at}}{k_B T}\right). \tag{1}$$

Here E_{at} is the effective reorientation energy barrier averaged over all possible paths, ρ is the areal density of the gas-phase molecules, p_a is a capture perimeter, $a = \sqrt{Q}$ is the capture width (linear dimension of molecules), and ν_{diff} is the thermal or effective hopping frequency of diffusing molecules. The rate of detachment is as follows:

$$R_{det} = \rho_l \nu\, p_A \exp(-E_{det}/k_B T). \tag{2}$$

Here ρ_l is the linear density of the solid-state molecules, ν is the statistical average frequency of the vibrational mode (in-plane lattice mode) responsible in detachment, and p_A is the perimeter of the island/cluster within an area of interest A_0. In the kinetic equilibrium, $R_{at} = R_{det}$. The normalized kinetic equilibrium concentration ρ/ρ_s at the steady state is as follows:

$$\rho_{\text{norm}}^{\text{incrp}} = \frac{\rho}{\rho_s} = \frac{2\nu\, p_A \rho_l}{\rho_s\, p_a \sqrt{\Omega}\nu_{\text{diff}}} \exp(-\Delta E/k_B T) = \frac{2\nu\, p_A}{p_a \nu_{\text{diff}}} \exp(-\Delta E/k_B T) \tag{3}$$

$\rho_s = \rho_l\sqrt{\Omega}$ is the areal density of the solid-state molecules just at an island edge or a normalization constant in the experiments. The difference $\Delta E = E_{det} - E_{at}$ is the energy barrier for molecule attachment. If the cluster size is large enough in comparison with the dimension of the molecule, which is the case for the observable size of clusters/islands in the LEEM mirror mode, the p_A/p_a is unity.

The incorporation-limited nucleation of a growing island, thus, does not only depend on a formation of a critical nucleus, but also requires reaching a critical concentration described by Eq. (3). Therefore a delayed observable nucleation occurs in this growth system, and upon a nominal deposition required to reach a kinetic equilibrium of gas-phase molecules and nucleated while in a classical nucleation and atomistic film growth mechanism, the nucleation of an island is stabilized by the formation of a critical nucleus.

In one of the experiments, after deposition of about a nominal 0.7 ML of ZnPc at a substrate temperature of 425 K and observing the nucleation of crystalline islands, we increased the substrate temperature to 500 K. The crystalline ZnPc islands gradually dissolved into the diffusive phase. After the substrate temperature was lowered again, we again observed the nucleation of the ZnPc islands. When cooling down further after observing nucleation without any additional deposition, islands continued to grow (see the Supplemental Material [36]) and the equilibrium concentration decreased as described by Eq. (3). Such heating-cooling cycles were repeated several times, and the final coverages of the ZnPc crystalline phase at certain temperatures were observed to be the same as the one before the first heating cycle.

We also have examined the temperature dependency of nominal coverage to initiate nucleation of an island driven by the additional deposition required to reach the kinetic equilibrium of gas-phase molecules with a critical nucleus. Just upon observing the onset of a growing island, the deposition was stopped, and the substrate temperature was increased to dissolve the crystalline island into a gas phase. Subsequently, the deposition was continued with an identical rate to observe the next onset of the nucleation of the growing island at this higher substrate temperature. This procedure has been repeated to obtain critical coverage data versus substrate temperature. We found that the delays in nucleation of the growing crystalline island for both phases $R33.69$ and 5×5 are associated with a nominal coverage needed to reach the kinetic equilibrium as described in Eq. (3). In Fig. 5 the relation between the critical coverage required for nucleation of crystalline islands and the growth temperature for both $R33.69$ and 5×5 phases is shown. The activation barrier determining the gas-phase concentration (the inset in Fig. 5) is

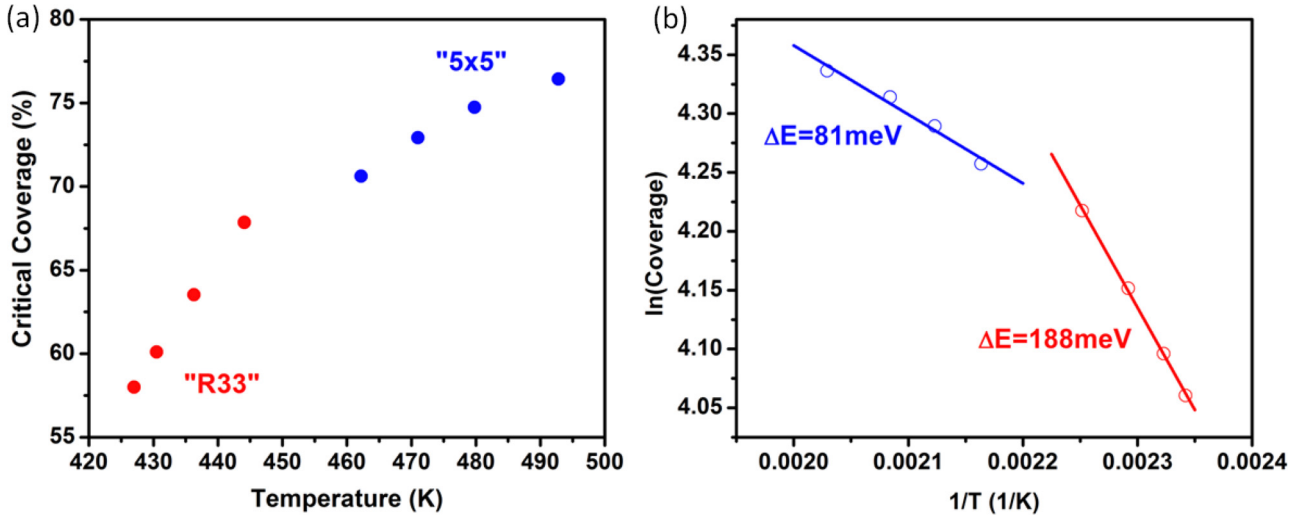

FIG. 5. (a) Critical coverage required for the nucleation of crystalline ZnPc islands at a given temperature for both *R*33.69 and 5 × 5 phases and (b) Arrhenius plots of the data with extracted values of effective bonding energies for each phase.

lower for the high-temperature phase (single crystalline, 5 × 5) than for the low-temperature phase (double-domain structure, *R*33.69).

As mentioned above, the 5 × 5 structure found at higher substrate temperatures is a substrate-induced single orientation commensurate phase, and it is less dense than the *R*33.69 phase. We searched for the possibilities of achieving a larger domain of the *R*33.69 phase at high temperatures, and we looked at what happened upon increasing coverage beyond 1 ML of the 5 × 5 phase. In some cases we observed partial conversion to the *R*33.69 phase, perhaps due to the inefficient rearrangement of azimuthally anisotropic molecules in the high coverage regime where the surrounding molecules are in close proximity. Interestingly, when we continue to grow ZnPc at temperatures at or above 475 K, the 5 × 5 film converts to the *R*33.69 phase when the nominal deposition reaches 1 ML (in terms of the molecular density of the *R*33.69 phase) as is evident from the μ-LEED patterns shown in Fig. 6. This further suggests that the 5 × 5 ZnPc structure is a substrate-induced phase and the *R*33.69 phase is more bulklike.

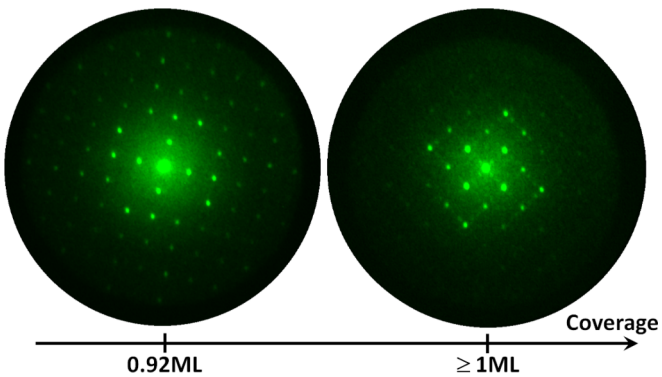

FIG. 6. μ-LEED patterns illustrating the phase transition from the 5 × 5 (left) to the *R*33.69 phase (right) at 460 K when the nominal coverage reaches 1 ML; weak satellite spots in the right pattern are from moiré modulation formed by overlapping ZnPc and Ag crystal lattices; electron energies are 25 and 23 eV, respectively.

In our LEEM experiments, although we could not observe the initial site of the start of phase transition, samples were swept along the *XY* position over 0.5 mm after observing phase transition in the μ-LEED mode in LEEM. On surfaces with initial higher defect densities, we found that both *R*33.69 domains are present with individual domain sizes in the range from about 10 μm to several hundred micrometers in diameter. With improving substrate quality, the individual domain sizes were larger—often approaching 0.5 mm. Therefore we conclude that the phase transition usually starts from substrate defects and thus the nucleation density of the *R*33.69 domains during the phase transition from the 5 × 5 structure is directly related to the initial substrate quality.

In the LEEM experiments we did not observe three-dimensional (3D) growth of ZnPc at RT up to 6 ML nominal deposition. But in this case, the single domain size of *R*33.69 is of submicrometer size only. However, at higher temperatures the well-ordered layer-by-layer growth is sustained only up to 2 ML. Above that thickness the ZnPc film becomes somewhat disordered with an appearance of 3D islands. Interestingly, when a giant *R*33.69 domain is grown at HTs via the phase transformation described above, it is stable upon cooling; further deposition of ZnPc on this giant ML *R*33.69 domain at low temperatures results in the layer-by-layer growth having an identical domain orientation as the first layer to at least 6 ML—a maximum thickness that we have studied in our current investigation so far.

IV. CONCLUSIONS

To summarize, we have reported here the film growth and coverage-/temperature-dependent phase-transition processes of ZnPc on a Ag(100) substrate observed in real-time LEEM and μ-LEED experiments complemented by the understanding of the interfacial energies obtained from DFT calculations. Our LEEM/LEED observation of film growth at substrate temperatures ranging from RT to 520 K revealed a delayed nucleation of crystalline ZnPc islands similar to those as reported for CuPc [23]. The temperature-dependent real-time concentration of gas-phase molecules determined from LEEM

experiments and computational support revealed that the kinetic equilibrium resulted from the balance of incorporation-limited slow attachment of molecules and thermal detachment from the island edge is responsible for such a delay in the nucleation of growing ML high two-dimensional islands. Upon continued deposition the crystalline phase continues to grow because of the excess deposition such that a high constant gas-phase concentration is maintained within interisland spaces. We observed the nucleation and growth of two crystalline phases. A double-domain structure with respect to the substrate surface lattice orientation (labeled *R*33.69) is grown below 440 K. This is similar to what was reported for ZnPc on Ag(100) in Ref. [22] and expected as the overlayers have a misorientation of lattice vectors with respect to the substrate and the nucleation density is high even at low flux typically used in our experiments (order of 0.05 ML/min). Another phase is a substrate-induced single-crystalline 5×5 commensurate structure when grown above that temperature, identical to one reported for CoPc grown at RT [21]. The in-plane density of molecules in the *R*33.69 structure is larger (in-plane molecule separation is by $\sim$4%) than the one in the 5×5 structure. Interestingly we have found that the selective nucleation and growth of the *R*33.69 and 5×5 structures are precisely tunable solely by maintaining a substrate temperature without choosing an alternate metal center and substrate for coverages below 1 ML. At higher temperatures, if the deposition of ZnPc molecules exceeds 1 ML, the single-crystalline 5×5 phase transforms irreversibly into the *R*33.69 one, which can have domain sizes of few tens to several hundred micrometers. Full elucidation of the underlying kinetic factors in the tuning of the structural phases (conformations) found in this material system requires further detailed study, but our findings provide an insight in the understanding of nucleation and growth of anisotropic organic molecules and can easily be extended on other similar phthalocyanine metal systems.

ACKNOWLEDGMENTS

We would like to thank P. Liu and G. Nintzel for technical support. This research used resources of the Center for Functional Nanomaterials and National Synchrotron Light Source, which are from the US DOE Office of Science User Facilities at Brookhaven National Laboratory under Contract No. DE-SC0012704.

[1] J. M. Gottfried, Surf. Sci. Rep. **70**, 259 (2015).
[2] R. A. Wassel and C. B. Gorman, Angew. Chem., Int. Ed. **43**, 5120 (2004).
[3] F. I. Bohrer, C. N. Colesniuc, J. Park, M. E. Ruidiaz, I. K. Schuller, A. C. Kummel, and W. C. Trogler, J. Am. Chem. Soc. **131**, 478 (2009).
[4] M. García-Iglesias, J.-J. Cid, J.-H. Yum, A. Forneli, P. Vázquez, M. K. Nazeeruddin, E. Palomares, M. Grätzel, and T. Torres, Energy Environ. Sci. **4**, 189 (2011).
[5] D. Dini and M. Hanack, 107-Physical Properties of Phthalocyanine-Based Materials, *The Porphyrin Handbook, Phthalocyanines: Properties and Materials*, edited by K. M. Kadish, R. Guilard, and K. M. Smith (Academic Press, Amsterdam, 2003), Vol. 17, pp. 1–36.
[6] O. L. Kaliya, E. A. Lukyanets, and G. N. Vorozhtsov, J. Porphyrins Phthalocyanines **3**, 592 (1999).
[7] W. Li, A. Yu, D. C. Higgins, B. G. Llanos, and Z. Chen, J. Am. Chem. Soc. **132**, 17056 (2010).
[8] A. Loas, R. Gerdes, Y. Zhang, and S. M. Gorun, Dalton Trans. **40**, 5162 (2011).
[9] T. A. Temofonte and K. F. Schoch, J. Appl. Phys. **65**, 1350 (1989).
[10] W. Gopel, Synth. Met. **41**, 1087 (1991).
[11] M. Bouvet, Anal. Bioanal. Chem. **384**, 366 (2006).
[12] J. Zhou and Q. Sun, J. Am. Chem. Soc. **133**, 15113 (2001).
[13] A. B. Sorokin, Chem. Rev. **113**, 8152 (2013).
[14] N. B. McKeown, *Phthalocyanine Materials* (Cambridge University Press, Cambridge, UK, 1998).
[15] A. Wilson and R. A. Collins, Sens. Actuators **12**, 389 (1987).
[16] S. Heutz, S. M. Bayliss, R. L. Middleton, G. Rumbles, and T. S. Jones, J. Phys. Chem. B **104**, 7124 (2000).
[17] A. Al-Mahboob, J. T. Sadowski, T. Nishihara, Y. Fujikawa, Q. K. Xue, K. Nakajima, and T. Sakurai, Surf. Sci. **601**, 1311 (2007).
[18] A. Al-Mahboob, J. T. Sadowski, Y. Fujikawa, K. Nakajima, and T. Sakurai, Phys. Rev. B **77**, 035426 (2008).
[19] J. T. Sadowski, G. Sazaki, S. Nishikata, A. Al-Mahboob, Y. Fujikawa, K. Nakajima, R. M. Tromp, and T. Sakurai, Phys. Rev. Lett. **98**, 046104 (2007).
[20] A. Al-Mahboob, Y. Fujikawa, T. Sakurai, and J. T. Sadowski, Adv. Funct. Mater. **23**, 2653 (2013).
[21] E. Salomon, P. Amsalem, N. Marom, M. Vondracek, L. Kronik, N. Koch, and T. Angot, Phys. Rev. B **87**, 075407 (2013).
[22] W. Dou, Y. Tang, C. S. Lee, S. N. Bao, and S. T. Lee, J. Chem. Phys. **133**, 144704 (2010).
[23] B. Stadtmüller, I. Kröger, F. Reinert, and C. Kumpf, Phys. Rev. B **83**, 085416 (2011).
[24] E. Bauer, Rep. Prog. Phys. **57**, 895 (1994).
[25] B. Delley, J. Chem. Phys. **92**, 508 (1990).
[26] B. Delley, J. Chem. Phys. **113**, 7756 (2000).
[27] J. P. Perdew, K. Burke, and M. Ernzerhof, Phys. Rev. Lett. **77**, 3865 (1996).
[28] S. Grimme, J. Comput. Chem. **27**, 1787 (2006).
[29] E. R. McNellis, J. Meyer, and K. Reuter, Phys. Rev. B. **80**, 205414 (2009).
[30] D. D. Koelling and B. N. Harmon, J. Phys. C: Solid State Phys. **10**, 3107 (1977).
[31] M. Douglas and N. M. Kroll, Ann. Phys. (San Diego) **82**, 89 (1974).
[32] B. Delley, Phys. Rev. B **66**, 155125 (2002).
[33] I. Kröger, B. Stadtmüller, C. Wagner, C. Weiss, R. Temirov, F. S. Tautz, and C. Kumpf, J. Chem. Phys. **135**, 234703 (2011).
[34] A. Al-Mahboob, Y. Fujikawa, J. T. Sadowski, T. Hashizume, and T. Sakurai, Phys. Rev. B **82**, 235421 (2010).
[35] A. Mugarza, R. Robles, C. Krull, R. Korytár, N. Lorente, and P. Gambardella, Phys. Rev. B **85**, 155437 (2012).
[36] See Supplemental Material at http://link.aps.org/supplemental/10.1103/PhysRevB.93.085413 for the observation of the growth of the islands.